Available online at www.sciencedirect.com

ScienceDirect

British Journal of Oral and Maxillofacial Surgery 57 (2019) 174–181

BRITISH Journal of Oral and Maxillofacial Surgery

www.bjoms.com

Intraoperative verification of resection margins of maxillary malignancies by cone-beam computed tomography

O. Ivashchenko [a,b,*,1], B. Pouw [a,1], J.K. de Witt [c], E. Koudounarakis [c], J. Nijkamp [a], R.L.P. van Veen [c], T.J.M. Ruers [a,d], B.M. Karakullukcu [c,**]

[a] *Department of Surgical Oncology, The Netherland Cancer Institute/Antoni van Leeuwenhoek Hospital, Amsterdam, The Netherlands*
[b] *Department of Radiology, Leiden University Medical Center, Leiden, The Netherlands*
[c] *Department of Head and Neck Oncology and Surgery, The Netherland Cancer Institute/Antoni van Leeuwenhoek Hospital, Amsterdam, The Netherlands*
[d] *MIRA Institute of Biomedical Technology and Technical Medicine, University of Twente, Drienerlolaan 5, 7522 NB Enschede, The Netherlands*

Available online 31 January 2019

Abstract

Resection of maxillary cancer often results in incomplete excision because of the tumour's proximity to important structures such as the orbit. To deal with this problem we prospectively investigated the feasibility of intraoperative imaging during maxillectomy to verify the planned resection margins. In total, six patients diagnosed with maxillary cancer listed for maxillectomy were included, irrespective of the histological type of tumour. Before resection, an accurate intended resection volume was delineated on diagnostic images. At the end of the operation we took a cone-beam computed tomographic (CT) scan of the treated maxilla, after which the accuracy of the resection was quantitatively evaluated by comparing the preoperative resection plan and the images acquired intraoperatively, based on the anatomy. Further resection was then done if necessary and quantitatively evaluated with a second cone-beam CT scan. Postoperatively we compared the results of the scan with those of the histological examination. Of the six, two resections were reported pathologically as less than radical, each of which was detected by intraoperative CT and resulted in extensions of the original resections. The mean (SD) distance between the planned and the actual resection was 1.49 (2.78) mm. This suggests that intraoperative cone-beam CT imaging is a promising way to make an adequate intraoperative assessment of planned surgical margins of maxillary tumours. This allows for intraoperative resection margins to be improved, possibly leading to a better prognosis for the patient.

Keywords: Cone-beam CT; Maxilla; Neoplasm; Margins of Excision; Computer-Assisted Surgery

Introduction

Maxillary malignant neoplasms are rare with an annual incidence of about 1/100,000 in most developed countries. That is less than 1% of all neoplasms, and less than 10% of those of the head and neck.[1–3] It is often difficult to identify the specific site of origin of large maxillary tumours because of the contiguity of the nasal cavities and the paranasal sinuses.

Standard examination consists of a computed tomographic (CT) scan with both bone and soft tissue windows. Next, magnetic resonance imaging (MRI) is useful for finding out the extent of the disease and for evaluation of the characteris-

* Corresponding author at: Department of Radiology, Leiden University Medical Center, Albinusdreef 2, 2333 ZA Leiden, The Netherlands. Tel: +31 71 526 3979.
** Corresponding author at: Department of Head and Neck Oncology and Surgery, The Netherland Cancer Institute, Antoni van Leeuwenhoek Hospital, Plesmanlaan 121, 1066 CX Amsterdam, The Netherlands. Tel: +31 205122558.
E-mail addresses: o.ivashchenko@lumc.nl (O. Ivashchenko), b.karakullukcu@nki.nl (B.M. Karakullukcu).
[1] Equal contribution.

https://doi.org/10.1016/j.bjoms.2019.01.007

tic perineural growth patterns.[4,5] Unfortunately, most cases present at an advanced stage with substantial tumour tissue invading the surrounding bony structures and sinuses, and resection is the mainstay of treatment for most of them.[6] However, the extent of tumour, lack of accurate up-to-date geometric information during resection, and the anatomical complexity, lead to a high rate of local failure postoperatively that ranges from 30% to 50%.[7,8] Survival in large series varies depending on the case mix, but in general, overall five-year survival of around 30%–50% has been reported.[3]

Image-guided surgery has many applications in head and neck surgery, ranging from the paranasal sinuses to the skull base and temporal bone where high precision image-guidance helps to avoid intraoperative damage of numerous critical structures.[9,10] Cone-beam CT has been used intraoperatively as an imaging tool during the management of facial fractures, orthognathic operations and resections of the temporal bone.[11–13] There is, however, to our knowledge only one feasibility study about the implementation of cone-beam CT in oncology of the head and neck. It concerns 12 cases (maxillectomy, mandibulectomy, and craniofacial resection) and indicates that intraoperative cone-beam CT has excellent spatial resolution and gives detailed bony definition, whereas soft tissue differentiation was rated as satisfactory.[14] Nonetheless, data about the value of intraoperative cone-beam CT in achieving tumour-free resection margins during surgery of the head and neck are lacking.

We have therefore investigated prospectively the clinical feasibility of using intraoperative cone-beam CT imaging to verify the intended resection margins during open maxillectomy for malignant neoplasms. We expected that because maxillary tumours are effectively embedded in the facial bones, it would be possible to evaluate the completeness of the resections within the maxilla based on intraoperative assessment of the bony structures that surround the tumour with cone-beam CT.

Material and methods

Intraoperative cone-beam CT scans were acquired with the Allura Xper FD20 X-ray system (Philips Healthcare), combined with a carbon "Magnus" table (Maquet) designed for intraoperative radiographic imaging. We also used an operating-theatre-compatible computer with an software developed in-house to analyse images for preparation of the virtual resection planning, viewing, and correlation of intraoperative cone-beam CT scans with corresponding virtual resection plans.

Study design

This prospective feasibility study was reviewed and approved by the local Medical Ethics Committee. Each patient provided written informed consent before inclusion in the study. As this was a pilot study, we did not do a power calculation on the sample size.

A total of six adult patients who had been diagnosed with maxillary malignancies and listed for open maxillectomy were included in the study. They all had stages T2-T4 (American Joint Committee on Cancer staging version 7) non-melanomas and squamous cell carcinomas (SCC), which reflected a typical group of patients at the time of resection.[8] They had all had CT and MRI preoperatively, after which a patient-specific virtual resection plan of the volume to be resected was created.

There were two phases of the study, the first of which focused on the development of the clinical workflow (cases 1-3), and the second which was the initial clinical evaluation of the method (cases 4-6). In the first phase, three patients had an intraoperative cone-beam CT scan at the end of the standard resection, but the scan was not applied further to the resection. Postoperatively we made a quantitative comparison of the virtual resection plan and the actual resection. During the second phase, patients had the same procedure as in phase I, but their resection planes could have been extended if the cone-beam CT had indicated that residual tumour was included in the virtual resection of that patient. The adequacy of the extended resection was verified with a second intraoperative scan.

Preoperative virtual resection planning

Patient-specific virtual resection plans were created preoperatively from CT and MRI scans. They were delineated semiautomatically by the operating surgeon, and contained detailed models of the skull, border of the tumour, and intended resection planes, with margins of about 10 mm from the border of the tumour. On the day of the operation this plan was discussed with the operating surgeon yet again, and shown on screens in the operating theatre to allow the surgeon to comply with the plan.

Operative stages

At the end of the initial resection, the cone-beam CT scanner was positioned around the head of the patient, while the scanner and the patient were covered with a sterile cover. Subsequently, radiographic projection data were acquired using the "XperCT Roll" protocol (119 kV, 202 mAs), and reconstructed on an isotropic 0.656 mm voxel grid.

Next, the reconstructed cone-beam CT scan was registered on the virtual resection plan containing a delineation picture of the tumour, planned resection planes, and the segmented skull. The registration of CT images was made using a rigid mutual-information-based algorithm, with a region of interest placed around the area of the resection. Subsequently, bony structures present in the scan were segmented and superimposed on the preoperative virtual resection plan, and Hausdorff distances between the remaining bony structure and the initial tumour or resection planes were calculated.

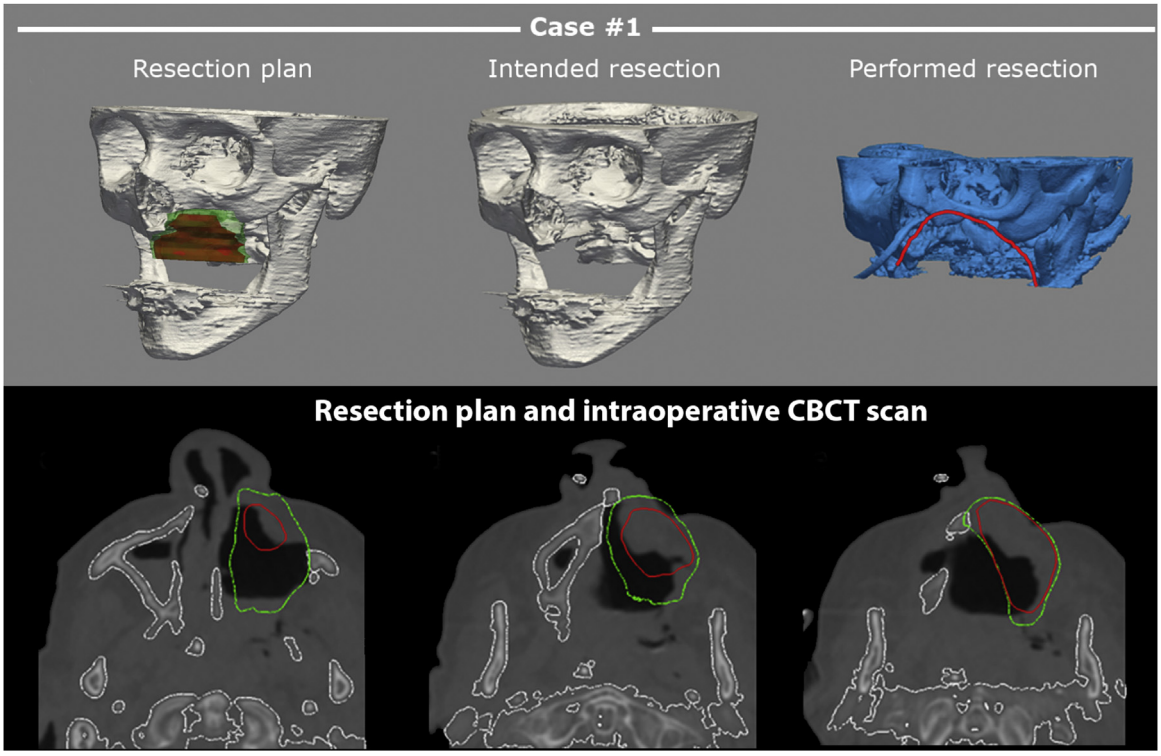

Fig. 1. Virtual resection plan for case 1 (left), showing delineated border of the tumour (red) and intended resection planes (green). This is followed by an "ideal" (that is, perfectly following the resection plan) and actual surgical resection, respectively. The lower row contains transverse slices of the intraoperative cone beam computed tomographic scan of the same patient, acquired at the end of the operation, and recorded on the resection plan.

The output could be seen as a 3-dimensional render and 2-dimensisonal slices with visible delineation contours (Fig. 1). If there was an overlap between the virtual resection plan and the remaining bones derived from the CT, we needed to extend the surgical resection (only in phase II). If the resection was extended, a second cone-beam CT was acquired for verification purposes.

Postoperative analysis of data

In operations on the head and neck, imaging-based correlation between the original volume of tumour and the resected part of soft tissue is hampered by low soft tissue contrast on intraoperative cone-beam CT and operation-related deformation and swelling of the tissue. To standardise quantitative assessment of resection volumes in this work, therefore, we decided to restrict analyses of the difference between the intended and the actual resection to borders of bony structures only.

For each patient, two measures of accuracy were calculated. The first, the Sørensen-Dice (Dice) similarity coefficient,[15] was used to calculate similarity in volume measured between the intended and the actually resected volumes of bone according to:

$$Dice = \frac{2 * |vol_{VRP} \cap vol_{true}|}{|vol_{true}| + |vol_{VRP}|} \quad (1)$$

where $|vol_{VRP}|$ is a "gold standard" volume, extracted as a result of the virtual resection planning, and $|vol_{true}|$ is the actually resected volume.

The second one, the signed Hausdorff distance (Hd),[16] is a surface-based measure that was used to extract distances between the actual bony resection and preoperatively measured surface of the tumour or bony resection planes. This measure illustrates inaccuracies in the surface of the volumes and is defined as:

$$H_d(X, Y) = max\left\{ \sup_{x \in X} \inf_{y \in Y} d(x, y), \sup_{y \in Y} \inf_{x \in X} d(x, y) \right\} \quad (2)$$

where $d(x, y)$ is the Euclidean distance and (x, y) are two points on two surfaces (X, Y) (for example, the planned, and the resected, bony volume).

Results

Phase I

For the three patients included in this phase the operation followed standard practice. Directly after the resection, a cone-beam CT scan of the resection area was acquired and registered to the virtual resection plan, which allowed us to compare the actual resected area with the planned area of resection.

Table 1
Comparison of the main outcomes of the study for phases one (cases 1–3) and two (cases 4–6).

Variable	Case 1	Case 2	Case 3	Case 4	Case 5	Case 6
Age (years)	86	72	52	82	55	80
Type of tumour	SCC	SCC	SCC	SCC	SCC	SCC (VC)
Stage	T4aN0M0	T4aN0M0	T4aN0M0	T4aN0M0	T4bN0M0	T2N0M0
Site of tumour	Left maxilla	Right maxillary sinus	Left processus alveolaris	Maxillary midline	Left maxillary sinus	Right processus alveolaris
Volume of tumour (cm^3)	16.4	5.8	28.3	12.9	11.1	2.3
Dice coefficient	0.87	0.78	0.95	0.49	0.69 0.76*	0.71
Hd* (mm)	2.92 (4.99)	1.68 (3.10)	0.04 (0.46)	2.93 (3.75)	0.65 (2.31) 1.55 (3.4)**	0.77 (2.09)
Hd_{min} (mm)	−12.32	−8.28	−4.46	−11.38	−11.25 −10.62**	−8.32

SCC = squamous cell carcinoma; VC = verrucous carcinoma.
* Hausdorff distance between intended and actual resection planes.
** After extension of the excision, verified with a second cone-beam CT scan.

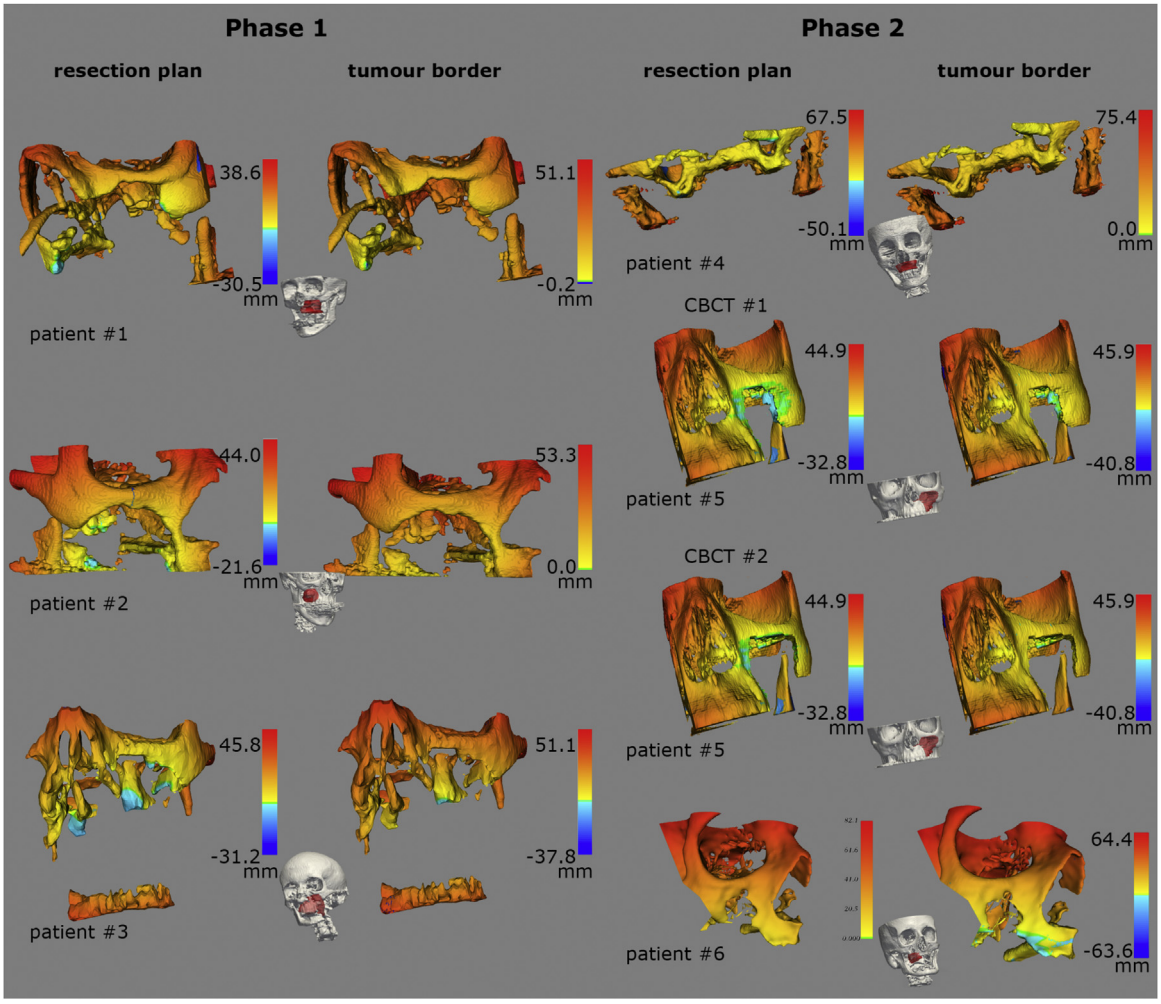

Fig. 2. The absolute distance between the remaining bony structures, extracted from the cone-beam computed tomographic scan that was acquired at the end of the operation, and the intended resection planes or preoperatively-defined border of the tumour, plotted as a colour map on the surface of the mesh.

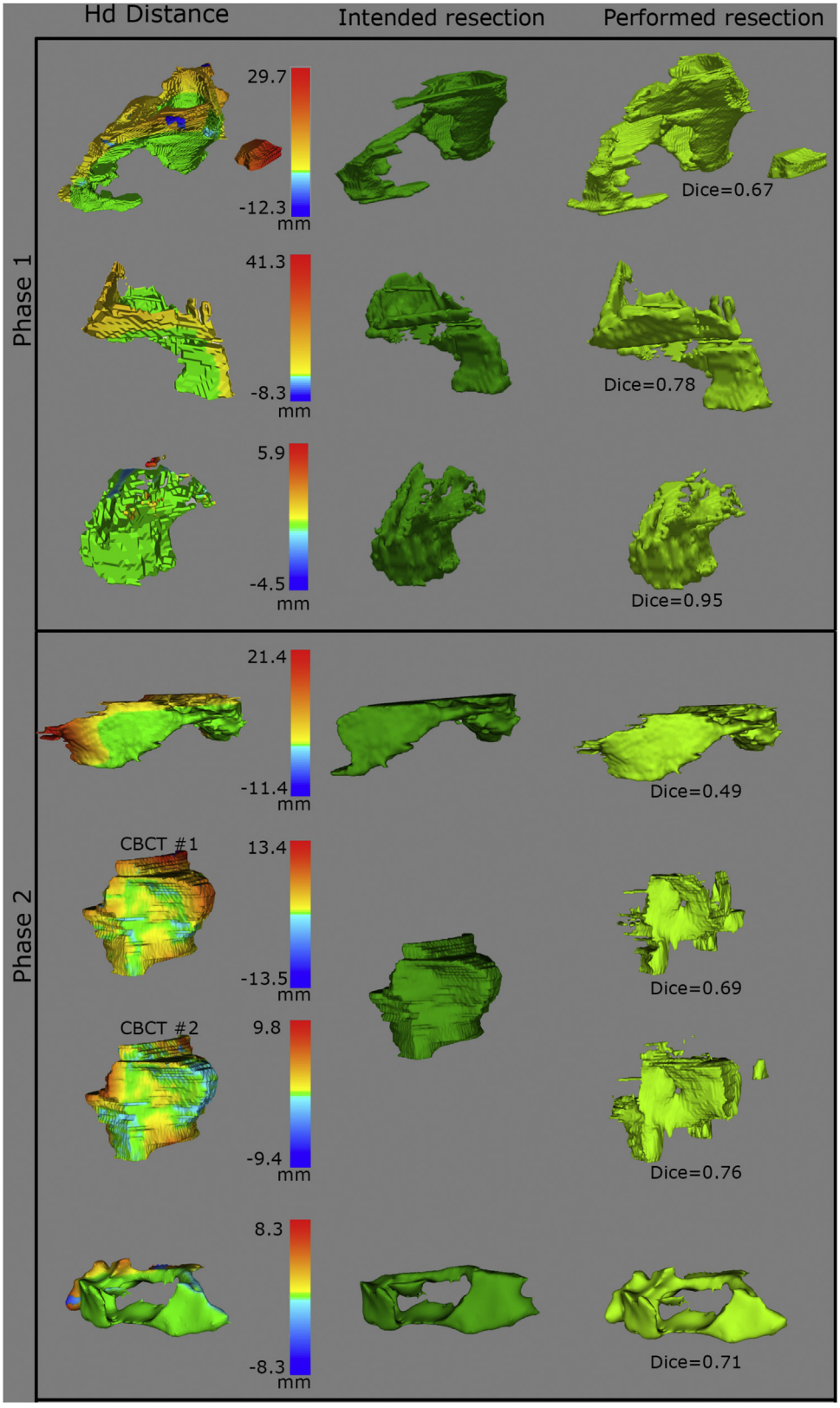

Fig. 3. Comparison of the intended and actually resected volumes of bone for Phase I and Phase II of the study. In the left hand column, is the signed Hausdorff distance between actually resected and planned volumes of bone, plotted as a colour map on the surface of the remaining bone. In this case, the light green colour of the mesh indicates complete correspondence between the planned and the actual resection, while the light-to-dark blue or yellow-to-red colours indicate under-resection and over-resection, respectively.

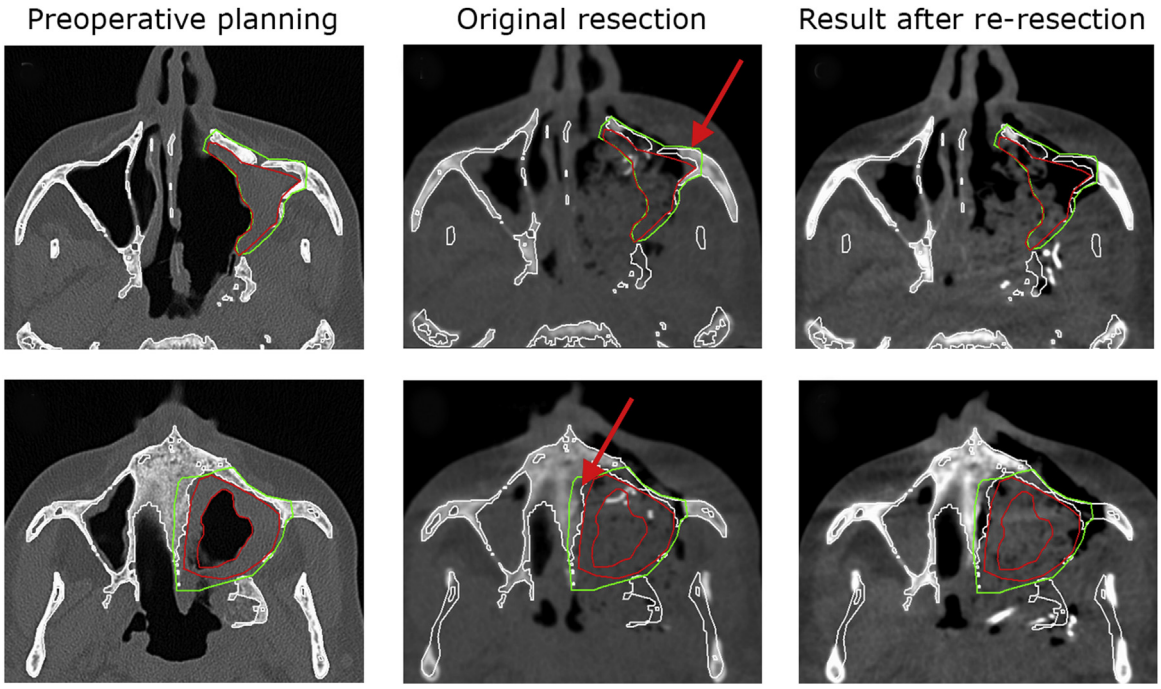

Fig. 4. Axial slices of case 5 with a squamous cell carcinoma in the left maxilla (white contour = bone, green = border of resection, red = border of tumour). Images show the original resection plan (left row), results of the initial resection assessed with the first cone-beam tomographic scan (middle row), and considerable undersection of bony structures preoperatively included in the resection plan, as well as the assessment of the extended resection with the second scan.

All patients in phase I of the study had squamous cell carcinomas, with or without a strong suspicion that the tumour had invaded the bones. The total volumes of tumour are shown in Table 1. Intraoperative cone-beam CT-based assessment of resection margins correlated with the histopathological evaluation in all patients.

In case 1, the intraoperative scan indicated that the medial side of the tumour had a resection margin that was less than that on the virtual plan (Fig. 1), indicating the possibility of invaded resection margins. However, because the patient was included in phase I of the study, we made no adjustment to the original resection. Postoperatively, pathological examination confirmed under-resection of the tumour, and the presence of zero resection margins at the medial border of the specimen.

The resections of cases 2 and 3 followed or exceeded their virtual planned excisions based on intraoperative assessment of the scans, and this was confirmed by histopathological examination.

Based on quantitative comparison of virtual and actual resections, the Dice coefficient was 0.87, 0.78 and 0.95, for cases 1, 2, and 3. The mean Hausdorff distance between the virtual plan and the part of the bone that was actually resected is shown in Table 1 and Fig. 2.

In phase I, all operative steps were finished within 10 minutes, including the sterile operative cone-beam CT scan, registration of the scan to the virtual plan, and assessment of planned resection margins on bony structures. Results of intraoperative assessments of the margins showed direct correlation with the histopathological picture, which indicating possible transition to phase II of the study.

Phase II

In the second phase, intraoperative cone-beam CT scans were assessed in real time, with the goal of finding out the minimal distance between the virtual plan and the actual resection planes.

Intraoperative cone-beam CT scans of cases 4 and 6 indicated clear resection margins, so no further excision was required. These results correlated with the pathological reports.

Case 5 showed smaller than intended margins at various sites (one medial and two ventral), which led to extension of the resections (Figs. 3 and 4). After the extension, a second cone-beam CT scan showed general improvement in the bony margins on the medial and one ventral side. However, there was still a smaller than intended resection margin at the second ventral location (Fig. 4) so the ventral margins were extended, and the operation ended. Because we had a limit of two intraoperative scans/patient in the protocol, no scan was acquired after the second extended resection. The pathology report confirmed invaded resection margins of the initial resection at three sides indicated by the first scan, and the report confirmed residual invasion of the resection margins on the ventral side of the secondary resection specimen.

The quantitative evaluations of cases in phase II by the Dice index are shown in Table 1 and Figs. 3 and 4.

Discussion

As the first step of the study, a detailed virtual resection plan that contained bony structures, tumour, and the intended resection border was created for each patient (Fig. 1). Subsequently, the resection was evaluated by comparing the actual resection planes with the original plan based on dissected bony structures (Figs. 2 and 4). If resection of bones included in the delineation of the tumour was incomplete, the borders were extended. Among the six patients reported here, two pathologically incomplete resections were reported, each of which was detected by intraoperative cone-beam CT (cases 1 and 5, Figs. 1 and 4).

The study design required intraoperative acquisition of a sterile cone-beam CT scan, which can extend the total duration of the procedure. However, we were able to fulfill all the intraoperative steps within 10 minutes, and with an acceptable radiation exposure of less than 2mSv.[17,18] We think that our work illustrates a promising method for detection of incompletely-resected tumours that allows for improvement of resection margins intraoperatively and may lead to a better prognosis for patients.[6,14,19,20]

The quantitative assessment of resections that is achieved with our method allows the surgeon to evaluate actual resections accurately. Although surgeons were trying to resect each tumour exactly according to the virtual plan, they achieved only a mean (SD) of 75% (15%) volume overlap between the planned and the actual resection. All the surgeons were surprised by the extent of the variations between their original plan and the actual excision, indicating that there is a need for image-guidance during oncological operations in the head and neck. Similar results have been encountered in interventional radiological applications of cone-beam CT scans.[21]

Because the soft tissue contrast was poor in the cone-beam CT images, all resections were analysed using bony structures only, while information about soft tissue margins was not available. Of course, evaluation of resection based on bony anatomy provides information only about the extent of the resection. Nevertheless, because maxillary malignancies are effectively embedded into facial bones, assessment of bony structures can provide sufficient guidance during resection.

Naturally, our method has a few limitations that affect the accuracy and, in some cases, clinical relevance of the method. First, accuracy of delineations used for preoperative surgical planning can be hampered by poor visualisation of the tumour on diagnostic images (such as artefacts from dental fillings). Secondly, accuracy of the method will be ultimately affected by interobserver variation of delineations as a result of manual segmentation of the tumours. Although this effect was not studied for surgical planning, various studies in radiotherapy have reported considerable interobserver variations in manually-defined treatment plans,[19,22] an effect that can be significantly reduced by automating the segmentation.[23,24]

Conclusion

Intraoperative cone-beam CT scans have shown that they can adequately detect inadequate resections margins in the maxilla, which will allow for immediate adjustment of the extent of the resection.

Conflict of interest

We have no conflicts of interest.

Ethics statement/confirmation of patients' permission

The study was done with the approval of the local Medical Ethics Committee, and is recorded in the ISRCTN trial register under number 14469511. Informed consent was obtained from each patient.

References

1. Qureshi SS, Chaukar DA, Talole SD, et al. Squamous cell carcinoma of the maxillary sinus: a Tata Memorial Hospital experience. *Indian J Cancer* 2006;**43**:26–9.
2. Guntinas-Lichius O, Kreppel MP, Stuetzer H, et al. Single modality and multimodality treatment of nasal and paranasal sinuses cancer: a single institution experience of 229 patients. *Eur J Surg Oncol* 2007;**33**:222–8.
3. Won HS, Chun SH, Kim BS, et al. Treatment outcome of maxillary sinus cancer. *Rare Tumors* 2009;**1**:e36.
4. Ariyoshi Y, Shimahara M. Magnetic resonance imaging of maxillary cancer — possibility of detecting bone destruction. *Oral Oncol* 2000;**36**:499–507.
5. Sakata K, Hareyama M, Tamakawa M, et al. Prognostic factors of nasopharynx tumors investigated by MR imaging and the value of MR imaging in the newly published TNM staging. *Int J Radiat Oncol Biol Phys* 1999;**43**:273–8.
6. van Doeveren TE, Karakullukcu MB, van Veen RL, et al. Adjuvant photodynamic therapy in head and neck cancer after tumor-positive resection margins. *Laryngoscope* 2018;**128**:657–63.
7. Kreeft AM, Smeele LE, Rasch CR, et al. Preoperative imaging and surgical margins in maxillectomy patients. *Head Neck* 2012;**34**:1652–6.
8. Hinni ML, Ferlito A, Brandwein-Gensler MS, et al. Surgical margins in head and neck cancer. A contemporary review. *Head Neck* 2012;**38**:1362–70.
9. Strauss G, Koulechov K, Richter R, et al. Navigated control in functional endoscopic sinus surgery. *Int J Med Robot* 2005;**1**:31–41.
10. Naujokat H, Rohnen M, Lichtenstein J, et al. Computer-assisted orthognathic surgery: evaluation of mandible registration accuracy and report of the first clinical cases of navigated sagittal split ramus osteotomy. *Int J Oral Maxillofac Surg* 2017;**46**:1291–7.
11. Chan Y, Siewerdsen JH, Rafferty MA, et al. Cone-beam computed tomography on a mobile C-arm: novel intraoperative imaging technology for guidance of head and neck surgery. *J Otolaryngol Head Neck Surg* 2008;**37**:81–90.

12. Rafferty MA, Siewerdsen JH, Chan Y, et al. Investigation of C-arm cone-beam CT-guided surgery of the frontal recess. *Laryngoscope* 2005;**115**:2138–43.
13. Erovic BM, Daly MJ, Chan HH, et al. Evaluation of intraoperative cone beam computed tomography and optical drill tracking in temporal bone surgery. *Laryngoscope* 2013;**123**:2823–8.
14. King E, Daly MJ, Chan H, et al. Intraoperative cone-beam CT for head and neck surgery: feasibility of clinical implementation using a prototype mobile C-arm. *Head Neck* 2013;**35**:959–67.
15. Dice LR. Measures of the amount of ecologic association between species. *Ecology* 1945;**26**:297–302.
16. Huttenlocher DP, Klanderman GA, Rucklidge WJ. Comparing images using the Hausdorff distance. *IEEE Trans Pattern Anal Mach Intell* 1993;**15**:850–63.
17. Ludlow JB, Davies-Ludlow LE, Brooks SL, et al. Dosimetry of 3 CBCT devices for oral and maxillofacial radiology: CB Mercuray, NewTom 3G and i-CAT. *Dentomaxillofac Radiol* 2006;**35**:392.
18. Motro M, Schauseil M, Ludwig B, et al. Rapid-maxillary-expansion induced rhinological effects: a retrospective multicenter study. *Eur Arch Otorhinolaryngol* 2016;**273**:679–87.
[19]. Volgger V, Betz CS. Photodynamic therapy in the upper aerodigestive tract. Overview and outlook. *J Biophotonics* 2016;**9**:1302–13.
20. Karakullukcu B, van Oudenaarde K, Copper MP, et al. Photodynamic therapy of early stage oral cavity and oropharynx neoplasms: an outcome analysis of 170 patients. *Eur Arch Otorhinolaryngol* 2011;**268**:281–8.
21. Abdel-Rehim M, Ronot M, Sibert A, et al. Assessment of liver ablation using cone beam computed tomography. *World J Gastroenterol* 2015;**21**:517–24.
22. Weltens C, Menten J, Feron M, et al. Interobserver variations in gross tumor volume delineation of brain tumors on computed tomography and impact of magnetic resonance imaging. *Radiother Oncol* 2001;**60**:49–59.
23. Gordon AR, Loevner LA, Shukla-Dave A, et al. Intraobserver variability in the MR determination of tumor volume in squamous cell carcinoma of the pharynx. *Am J Neuroradiol* 2004;**25**:1092–8.
24. Njeh CF. Tumor delineation: the weakest link in the search for accuracy in radiotherapy. *J Med Phys* 2008;**33**:136–40.